

PAPER • OPEN ACCESS

Balancing hydrophobic and electrostatic interactions in thermosensitive polyplexes for nucleic acid delivery

To cite this article: Lies A L Fliervoet *et al* 2019 *Multifunct. Mater.* **2** 024002

View the [article online](#) for updates and enhancements.

Recent citations

- [Structure and Dynamics of Thermosensitive pDNA Polyplexes Studied by Time-Resolved Fluorescence Spectroscopy](#)
Lies A. L. Fliervoet *et al*

Multifunctional Materials



PAPER

Balancing hydrophobic and electrostatic interactions in thermosensitive polyplexes for nucleic acid delivery

OPEN ACCESS

RECEIVED
3 July 2018

REVISED
12 March 2019

ACCEPTED FOR PUBLICATION
25 March 2019

PUBLISHED
7 May 2019

Original content from this work may be used under the terms of the [Creative Commons Attribution 3.0 licence](#).

Any further distribution of this work must maintain attribution to the author(s) and the title of the work, journal citation and DOI.



Lies A L Fliervoet, Cornelus F van Nostrum, Wim E Hennink and Tina Vermonden¹

Department of Pharmaceutics, Utrecht Institute for Pharmaceutical Sciences, University of Utrecht, PO Box 80082, 3508 TB Utrecht, The Netherlands

¹ Mailing address: Department of Pharmaceutics, Utrecht Institute for Pharmaceutical Sciences, Utrecht University, Universiteitsweg 99, 3584 CG Utrecht, The Netherlands

E-mail: T.Vermonden@uu.nl

Keywords: plasmid DNA, ABC triblock copolymers, N-isopropylacrylamide (NIPAM), 2-(dimethylamino)ethyl methacrylate (DMAEMA), stimuli-responsive polymers, gene delivery

Supplementary material for this article is available [online](#)

Abstract

For the design of new polymeric-based drug delivery systems, understanding how multiple functionalities in the polymer structure are influencing each other in particle formation is important. Therefore in this study, the balance between hydrophobic and electrostatic interactions has been investigated for thermosensitive plasmid DNA (pDNA)-loaded polyplexes. NPD triblock copolymers consisting of a thermosensitive poly(N-isopropylacrylamide) (PNIPAM, N), a hydrophilic poly(ethylene glycol) (PEG, P) and a cationic poly(2-(dimethylamino)ethyl methacrylate) (PDMAEMA, D) block with different block lengths were prepared using a hetero-functional PEG macroinitiator. Cloud points of the thermosensitive polymers in HBS buffer (20 mM HEPES, 150 mM NaCl, pH 7.4) were determined by light scattering and ranged between 33 °C and 34 °C for the different polymers. The binding and condensation properties of these thermosensitive polymers and pDNA were studied taking non-thermosensitive PD polymers as controls. The size, surface charge, and stability of the formed colloidal particles ('polyplexes') were studied as a function of polymer block lengths, N/P charge ratio, and temperature. The NPD polymers were able to self-assemble into polyplex nanostructures with hydrodynamic sizes ranging between 150 and 205 nm at room temperature in HBS buffer as determined by dynamic light scattering. Polyplexes prepared with a low N/P charge ratio of 1 aggregated upon heating to 37 °C, which was not observed at higher N/P charge ratios. When the length of the cationic D block was relatively long compared to the thermosensitive N block, stable polyplexes were formed at all N/P ratios and elevated temperatures. ¹H-NMR studies, static light scattering and ζ -potential measurements further supported the stability of these polyplexes at 37 °C. Finally, the presence of thermosensitive blocks in NPD-based polyplexes resulted in better cytocompatibility compared to PD-based polyplexes with similar efficiencies of delivering its cargo into HeLa cells.

1. Introduction

Gene therapy is a field of research that emerged already a few decades ago, in which nucleic acid-based therapeutics are used to modulate cellular expression levels of specific genes and their functional proteins. However, widespread applications are still hampered by the difficulties to deliver the highly charged and large nucleic acid molecules to their intracellular targets, indicating the requirement of an advanced delivery system [1, 2]. Complexation of nucleic acids with polymeric carriers into polyplexes, is nowadays a recognized approach to facilitate the delivery and uptake by the target cells. The rationale to use these polymeric materials for gene delivery, is that cationic polymers are able to efficiently condense the negatively charged nucleic acids by electrostatic interactions into a polymer-nucleic acid complex, also named polyplexes [3]. A large number of

different cationic polymers have been developed and investigated as nucleic acid carriers, including polyethylenimine (PEI), poly-L-lysine (PLL), polyamidoamine (PAMAM), and poly(2-dimethylaminoethyl methacrylate) (PDMAEMA) [4, 5].

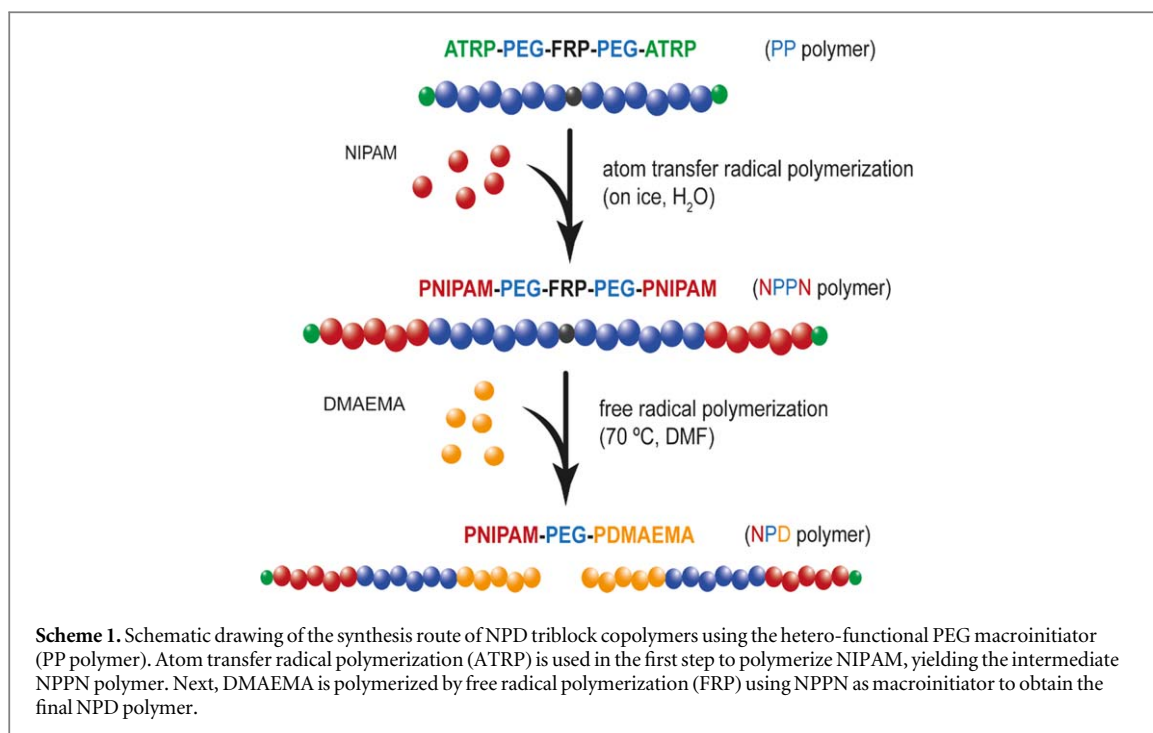
One of the advantages of using synthetic polymers, is the ability to control the chemical structure and composition to tailor the properties for specific applications. Block copolymers with well-defined architectures are an extensively studied category, since various multiphase structures on a nano- and macroscale can be formed when two or more polymeric blocks, having different physical properties, are covalently linked to each other [6]. Moreover, stimuli-responsive block copolymers form an interesting class of block copolymers because their self-assembly behavior can be influenced by biological or external physical triggers [7, 8]. Especially thermosensitive block copolymers have shown to be attractive for the preparation of materials for biomedical and pharmaceutical applications [9–12]. They undergo a phase transition from a soluble state to an insoluble state in aqueous solutions at a certain temperature. A well-studied polymer in this class is poly(*N*-isopropylacrylamide) (PNIPAM), because it has a lower critical solution temperature (LCST) in water of approximately 32 °C which is very close to body temperature [13]. Combining multiple stimuli-responsive groups into a polymer design, such as pH- and thermosensitivity, is an attractive approach to further improve nucleic acid delivery [14, 15]. For example, random copolymers of DMAEMA and NIPAM were studied as potential carriers for nucleic acids [16]. In addition, Kurisawa *et al* showed that DNA binding and transfection were enhanced by introducing the hydrophobic comonomer butylmethacrylate into P(NIPAM-*co*-DMAEMA) [17, 18]. The group of Alexander compared complex formation of branched PEI grafted with PNIPAM blocks with random copolymers of P(NIPAM-*co*-DMAEMA) and found higher DNA affinities above the LCST with the branched PEI-*g*-PNIPAM polymers [19, 20]. This finding may also suggest that separation of the multiple functionalities, electrostatic and thermosensitive, in the polymer by using block copolymers instead of random copolymers could further improve the polyplex properties. Furthermore, PNIPAM-based block copolymers have extensively been studied to develop ‘smart’ polymer gels since they can form a hydrogel network upon a temperature trigger [12, 21]. For example, such systems were investigated for the controlled-release of vascular endothelial growth factor (VEGF) [22] and drug-loaded micelles [23]. Recently, hydrogels have also been developed to facilitate local and sustained release of nucleic acids to reduce side effects and increase *in vivo* efficacy [24, 25]. Besides cationic and thermosensitive blocks, the use of block copolymers containing non-charged hydrophilic blocks as well has been described to provide a protective layer of hydrophilic domains on the surface of the polyplexes to increase their stability and biocompatibility *in vivo* [3, 5]. The macromolecule poly(ethylene glycol) (PEG) has been widely used as shielding polymer block, and the corresponding polyplexes indeed showed improved stability and reduced aspecific interactions with negatively charged biomolecules [26, 27].

Understanding how multiple functionalities in the polymer structure are influencing each other in DNA polyplex formation is essential in the design of new controlled-release systems. The stability and dynamics of polyplexes depend on the architecture and composition of the block copolymer [3, 14, 28], and optimizing the thermosensitive/electrostatic balance of the polymers might offer a way to fine-tune these properties. In this study, we first report the preparation of various linear NPD triblock copolymers consisting of a thermosensitive PNIPAM (N), an hydrophilic PEG (P) and a cationic PDMAEMA (D) block using a recently reported hetero-functional PEG macroinitiator [29]. Secondly, the *in vitro* behavior of these thermosensitive polymers in the formation of plasmid DNA (pDNA)-based polyplexes was compared with non-thermosensitive polymers. The size, surface charge, and stability of the polyplexes formed are studied as a function of polymer block composition and length, charge ratio, and temperature. This work aims at investigating how electrostatic and temperature-induced hydrophobic interactions are influencing each other and providing new insights for the design of polymers for advanced nucleic acid delivery systems.

2. Materials and methods

2.1. Materials

All materials were obtained from Sigma-Aldrich (Zwijndrecht, the Netherlands) and used as received unless noted otherwise. α -t-Butyloxycarbonylamino- ω -hydroxy poly(ethylene glycol) with PEG molecular weight of 5000 Da (Boc-NH-PEG₅₀₀₀-OH) was obtained from Iris Biotech GmbH (Marktredwitz, Germany) and dried overnight in a vacuum oven at room temperature (RT) before use. 4-(Dimethylamino)pyridinium-4-toluene-sulfonate (DPTS) was prepared according to a literature procedure [30]. Triethylamine (TEA) and 2,4,6-trinitrobenzene sulfonic acid (TNBSA) solution (5% w/v) were obtained from Thermo Fisher Scientific (Bleiswijk, the Netherlands). Peptide grade dichloromethane (DCM), *N,N*-dimethylformamide (DMF), tetrahydrofuran (THF) and diethyl ether were purchased from Biosolve (Valkenswaard, the Netherlands). All solvents were dried by molecular sieves for 24 h before use. To remove the inhibitor, 2-(dimethylamino)ethyl methacrylate (DMAEMA) was passed through a column of alumina prior to use. Slide-A-lyzer™ Dialysis



cassettes (Mw cut-off: 3500–10,000 Da) were obtained from Thermo Fisher Scientific (Bleiswijk, the Netherlands). The pGL3-control reporter vector, encoding for firefly luciferase, with simian virus 40 (SV40) promoter was purchased from Promega (Leiden, the Netherlands). The plasmid (5256 bp) was amplified with DH5 $_{\alpha}$ competent *E. coli* bacteria cells and purified using NucleoBond[®] PC2000 DNA purification (Macherey-Nagel, Bioke, Leiden, the Netherlands). Linear polyethylenimine (L-PEI, Mw 25,000 Da) was obtained from Polysciences (Hirschberg an der Bergstraße, Germany), agarose multi-purpose was purchased from Roche Molecular Biochemicals (Mannheim, Germany) and DNA Loading Dye from Fermentas (St. Leon-Roth, Germany). Midori Green DNA gel stain was obtained from Nippon Genetics (Dueren, Germany). Human epithelial ovarian carcinoma cells (HeLa) were originally obtained from the American Type Culture Collection (Maryland, USA). Luciferase assay kit and CellTiter 96[®] AQueous One Solution Cell Proliferation Assay (MTS) kit were purchased from Promega (Leiden, the Netherlands).

2.2. Synthesis of NPD triblock copolymers

The synthesis of the hetero-functional PEG macroinitiator ((Br-C(CH₃)₂-CO-NH-PEG₅₀₀₀)₂-ABCPA) was performed according to a three-step synthesis route as previously reported [29]. The PEG macroinitiator contains both an atom transfer radical polymerization (ATRP) initiator as an azoinitiator for classical free radical polymerization (FRP), namely 4,4'-azobis(4-cyanopentanoic acid) (ABCPA). NPD triblock copolymers, having various block lengths of PNIPAM (N) and PDMAEMA (D), were synthesized following a two-step procedure. The first step involved atom transfer radical polymerization followed by free radical polymerization (FRP) (scheme 1).

2.2.1. Synthesis of PNIPAM-PEG-PEG-PNIPAM (NPPN) polymers by atom transfer radical polymerization (ATRP)

The PEG macroinitiator (1 equiv.), NIPAM (283 or 566 equiv.) and CuBr (8 equiv.) were dissolved in water (3.5 or 7.0 ml) in an airtight screw-cap glass vial with a final NIPAM concentration of 90 mg ml⁻¹. The reaction mixture was flushed with nitrogen for 15 min at RT and subsequently another 15 min on ice. The reaction was started by adding 18 equiv. of tris[2-(dimethylamino)ethyl]amine (Me₆TREN), which changed the color of the mixture immediately from colorless to blue/green. The polymerization reaction was carried out for three hours on ice. Next, the polymer solution was transferred into a dialysis cassette and dialyzed against water for 48 h at 4 °C (Mw cut-off: 10 kDa), while changing the dialysate frequently (three times a day). Finally, the resulting NPPN polymer was recovered by freeze drying with a typical yield of 80%–90% and analyzed by ¹H-NMR spectroscopy and GPC.

2.2.2. Synthesis of PNIPAM-PEG-PDMAEMA (NDP) polymers by free radical polymerization (FRP)

The NPPN polymer (1 equiv.) and various amounts of the DMAEMA monomer (ranging from 396–1011 equiv.) were dissolved in dry DMF (ranging from 1–2 ml) in an airtight Schlenk flask with a final DMAEMA concentration of

300 mg ml⁻¹. At least three freeze-pump-thaw cycles were applied to degas the solution, after which the reaction mixture was placed in an oil bath at 70 °C and stirred for 24 h under N₂ atmosphere. The polymer solution was transferred into a dialysis cassette (Mw cut-off: 10 kDa) and dialyzed against water for 48 h at 4 °C, while changing the dialysate frequently (three times a day). The final NPD polymer was recovered by freeze drying with a typical yield of 65%–70%. Non-thermosensitive PD polymers, lacking the PNIPAM block, were synthesized as a control. For this, a PEG macroinitiator without ATRP initiator (Boc-NH-PEG₅₀₀₀)₂-ABCPA (1 equiv.) together with various amounts of DMAEMA (ranging from 391–692 equiv.) were dissolved in dry DMF and subjected to the same steps as described above. The synthesized polymers were analyzed by ¹H-NMR spectroscopy and GPC, and the cloud point (CP) was determined for thermosensitive polymers.

2.3. ¹H-NMR spectroscopy

The macroinitiator and polymers were characterized with ¹H-NMR spectroscopy on an Agilent 400 MR-NMR spectrometer (Agilent Technologies, Santa Clara, CA, USA). Polyplexes were analyzed on a Bruker 500 MHz NMR spectrometer at 10 and 40 °C in buffered D₂O (137 mM NaCl, 2.7 mM KCl, 11.9 mM phosphates, pH 7.4). Chemical shifts are referred to the residual solvent peak ($\delta = 7.26$ ppm for CDCl₃ and $\delta = 4.80$ ppm for D₂O). Data analysis was performed using MestReNova Software version 10.0.1-14 719.

2.4. Gel permeation chromatography (GPC)

The obtained polymers were characterized by GPC using a Waters Alliance System (Waters Corporation, Milford, MA, USA) equipped with a refractive index detector and a PLgel 5 μ M MIXED-D column (Polymer Laboratories) using DMF containing 10 mM LiCl as eluent. Polymer concentration was 3 mg ml⁻¹ and 50 μ l was injected into the column. The column temperature was set to 65 °C and the flow rate to 1.0 ml min⁻¹. Calibration was performed using PEG standards of narrow and defined molecular weights. Data analysis was performed using Empower 3 Software 2010.

2.5. Determination of cloud point (CP) of thermosensitive polymers

The CP of thermosensitive polymers was determined by light scattering using a Jasco FP-8300 spectrophotometer (JASCO, Easton, MD). The polymers were dissolved overnight at a concentration of 2 mg ml⁻¹ in 20 mM *N*-(2-hydroxyethyl)piperazine-*N'*-(2-ethanesulfonic acid) (HEPES) buffer, pH 7.4. Next, 1 ml of the polymer solution was transferred into a clean glass cuvette and the scattering intensity was measured at 550 nm while increasing the temperature from 10 °C to 60 °C with a heating rate of 1 °C min⁻¹. The CP was taken as the onset point of increasing scattering intensity.

2.6. Particle preparation

Polymer stock solutions (ranging from 40–939 μ g ml⁻¹, depending on polymer type and intended N/P ratio) and pDNA stock solution (150 μ g ml⁻¹) were prepared in HEPES buffer (20 mM HEPES, pH 7.4) and pre-cooled at 0 °C. The use of HEPES buffered aqueous solutions for the preparation of the polyplexes is a standard method reported in literature [31]. Subsequently, 600 μ l polymer solution was added to 300 μ l pDNA solution, and the mixture was vortexed for 10 s. The polyplexes, with a final pDNA concentration of 50 μ g ml⁻¹, were allowed to form at 0 °C for 30 min before further use. For the preparation of polyplexes above the CP of the NPD-polymers, all stock solutions were pre-warmed at 37 °C before mixing and incubated at 37 °C for 30 min to allow for polyplex formation. Micelles, without the addition of pDNA, were formed by rapidly heating the NPD-polymer solutions (1 mg ml⁻¹) to 37 °C and incubating for 15 min. For polyplex characterization by ¹H-NMR spectroscopy, buffered deuterated-water (137 mM NaCl, 2.7 mM KCl, 11.9 mM phosphates, pH 7.4) was used during the preparation.

2.7. Dynamic light scattering (DLS)

DLS was used to determine the hydrodynamic size and polydispersity index (PDI) of the polyplexes. The measurements were performed on an ALV CGS-3 system (Malvern Instruments, Malvern, UK) with a JDS Uniphase 22 mW He–Ne laser operating at 632.8 nm, an optical fiber-based detector, a digital LV/LSE-5003 correlator with temperature controller set at 4 °C, 25 °C, or 37 °C. Polyplexes for DLS analysis were prepared as described in section 2.6 and then diluted with concentrated HBS buffer to yield a final NaCl concentration of 150 mM and a final pDNA concentration of 20 μ g ml⁻¹. Measurements were analyzed corrected for viscosity at the different temperatures using the ALV-5000/E/EEP & ALV-60 \times 0 4.0 software.

2.8. Laser Doppler electrophoresis (LDE)

The ζ -potential of the polyplexes was measured using laser Doppler electrophoresis on a Zetazizer Nano-Z (Malvern Instruments). Samples were measured in HEPES buffer (20 mM HEPES, pH 7.4) at a final pDNA concentration of $20 \mu\text{g ml}^{-1}$.

2.9. Agarose gel retardation assay

Polyplexes prepared with different NPD- or PD-polymers at various N/P ratios were prepared as described in section 2.6. Polyplex dispersions were diluted with concentrated HBS buffer to yield a final NaCl concentration of 150 mM and a final pDNA concentration of $20 \mu\text{g ml}^{-1}$. Next, $20 \mu\text{l}$ of the polyplex sample was mixed with $4 \mu\text{l}$ heparin sodium salt solution (50 mg ml^{-1}) or $4 \mu\text{l}$ HBS buffer and incubated for 1 h at RT. Afterwards, $4 \mu\text{l}$ of loading dye was added to the mixture and loaded into a 0.8% agarose gel containing Midori Green in a tris-acetate-EDTA (TAE) buffer. The gel was run at 35 V for 40 min and analyzed by a Gel Doc XR + system (Bio-Rad Laboratories Inc., Hercules, CA) equipped with Image Lab software.

2.10. Static light scattering (SLS)

The radius of gyration and hydrodynamic radius of the polyplexes were determined by SLS using an ALV7004 correlator, ALV/LSE-5004 Goniometer, ALV/Dual High QE APD detector unit with fiber splitting device with a setup of 2 off detection system and a Uniphase Model 1145 P He–Ne Laser. The laser wavelength and power were set to 632.8 nm and 22 mW, respectively, and the temperature was controlled by a Julabo CF41 Thermostatic bath.

2.11. *In vitro* transfection and cytotoxicity studies

In vitro studies were performed according to the recommendations as previously described [31]. HeLa cells were cultured in Dulbecco's Modified Eagle's Medium (DMEM) with high glucose (4.5 g l^{-1} glucose) supplemented with 10% fetal bovine serum (FBS) at 37°C in a humidified atmosphere containing 5% CO_2 . Transfection studies were done in 96-well plates, with HeLa cells seeded at a density of 8000 cells/well 24 h before transfections. At the day of the experiment, cells were washed once with PBS and incubated with pDNA-loaded polyplexes (0.50 and $0.75 \mu\text{g pDNA/well}$) in complete medium for 6 h at 37°C . As a positive control for nucleic acid delivery, l-PEI (25 kDa) was used at an optimal N/P ratio of 6 [31]. Each condition was measured in octuple. Afterwards, transfection mixtures were replaced by fresh medium and plates were incubated for 24 h at 37°C . The following day, cells were lysed with $100 \mu\text{l}$ lysis buffer (25 mM Tris, 2 mM DTT, 2 mM DCTA, 1% Triton X-100, 10% glycerol) on a shaking board at RT for 15 min. Subsequently, $50 \mu\text{l}$ of lysate was transferred into a white luminescence plate and mixed with $50 \mu\text{l}$ of Luciferase Assay Reagent. Reagent was injected using a FLUOstar OPTIMA microplate reader (BMG Labtech, Ortenberg, Germany) equipped with an injection pump. Two seconds after injection, luminescence was measured for ten seconds according to supplier's recommendation. To assess the cytotoxicity of the tested formulations, an MTS assay was performed in parallel on a separate plate. The transfection protocol was similar as described above, but instead of adding lysis buffer, $100 \mu\text{l}$ fresh medium was added to each well followed by $20 \mu\text{l}$ MTS Assay Reagent. After 1–2 h incubation at 37°C , the absorbance at 490 nm and 690 nm was measured using the iMark™ Microplate Absorbance Reader (Bio-Rad Laboratories Inc., Hercules, CA) and cell viability was calculated relative to untreated cells.

3. Results and discussion

3.1. Synthesis and characterization of NPD triblock copolymers

The hetero-functional PEG macroinitiator was synthesized according to a three-step synthesis route, as reported before (scheme S1, table S1 is available online at stacks.iop.org/MFM/2/024002/mmedia) [29]. NPD triblock copolymers with different block lengths were synthesized following a two-step synthesis route (scheme 1). In the present study, NPD polymers consisting of a PEG midblock, flanked by blocks of PNIPAM and PDMAEMA to introduce thermosensitive and cationic properties to the polymer structure, respectively, were synthesized and characterized (figure 1(a)). The first block, consisting of PNIPAM, was polymerized by ATRP and the corresponding NPPN polymers ($N = \text{PNIPAM}$, $P = \text{PEG}$) were obtained with a monomer conversion ranging from 85%–94% based on $^1\text{H-NMR}$ analysis and a typical yield of 81%–90% (table S2). GPC analysis shows that the peak of the macroinitiator (14 min) was almost completely shifted to lower retention times (11–12 min), which corresponds to a higher M_n of the formed polymer (table 1) and thus confirmed the successful synthesis of the NPPN polymers. In the second step of the synthesis route, DMAEMA was polymerized by classical FRP to yield the final NPD ($N = \text{PNIPAM}$, $P = \text{PEG}$, $D = \text{PDMAEMA}$) triblock copolymers (table 1). Typically, the monomer conversion was 70%–80% as determined with $^1\text{H-NMR}$ (figure S1), and the different polymers were obtained in a yield ranging from 60%–75%. The characteristics of the synthesized polymers are shown in table 1.

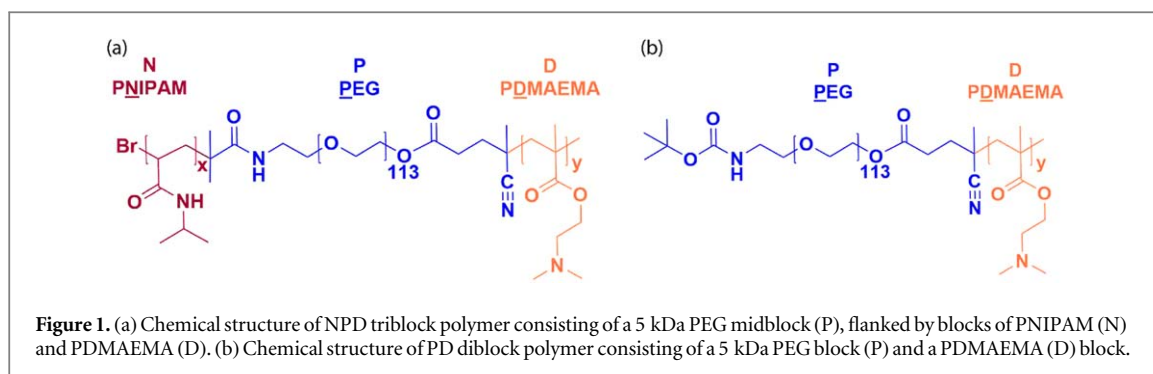


Table 1. Characteristics of various NPD triblock and PD diblock copolymers synthesized by radical polymerization using the hetero-functional PEG macroinitiator. The polymer names are abbreviated according to the block composition (N = PNIPAM, P = PEG, D = PDMAEMA).

Name	Feed initiator: monomer ratio mol/mol (N block)	Feed initiator: monomer ratio mol/mol (D block)	M_n N block (kDa) ^a	M_n P block (kDa) ^a	M_n D block (kDa) ^a	Total M_n (kDa) ^a	Total M_n (kDa) ^b	PDI ^b	Cloud Point (°C) ^c
N ₂₇ P ₅ D ₂₀	1:566	1:498	27	5	20	52	49	2.5	34
N ₂₇ P ₅ D ₄₃	1:566	1:789	27	5	43	75	83	1.8	34
N ₂₇ P ₅ D ₅₆	1:566	1:983	27	5	56	88	62	2.1	34
N ₁₅ P ₅ D ₂₀	1:283	1:396	15	5	20	40	46	2.1	33
N ₁₅ P ₅ D ₃₃	1:283	1:481	15	5	33	53	54	1.8	34
N ₁₅ P ₅ D ₄₃	1:283	1:789	15	5	43	63	51	1.8	34
N ₁₅ P ₅ D ₆₄	1:283	1:1011	15	5	64	84	62	1.8	34
P ₅ D ₁₉	n.a.	1:391	n.a.	5	19	24	20	1.8	n.a.
P ₅ D ₄₇	n.a.	1:692	n.a.	5	47	52	27	2.1	n.a.

^a Determined by ¹H-NMR.

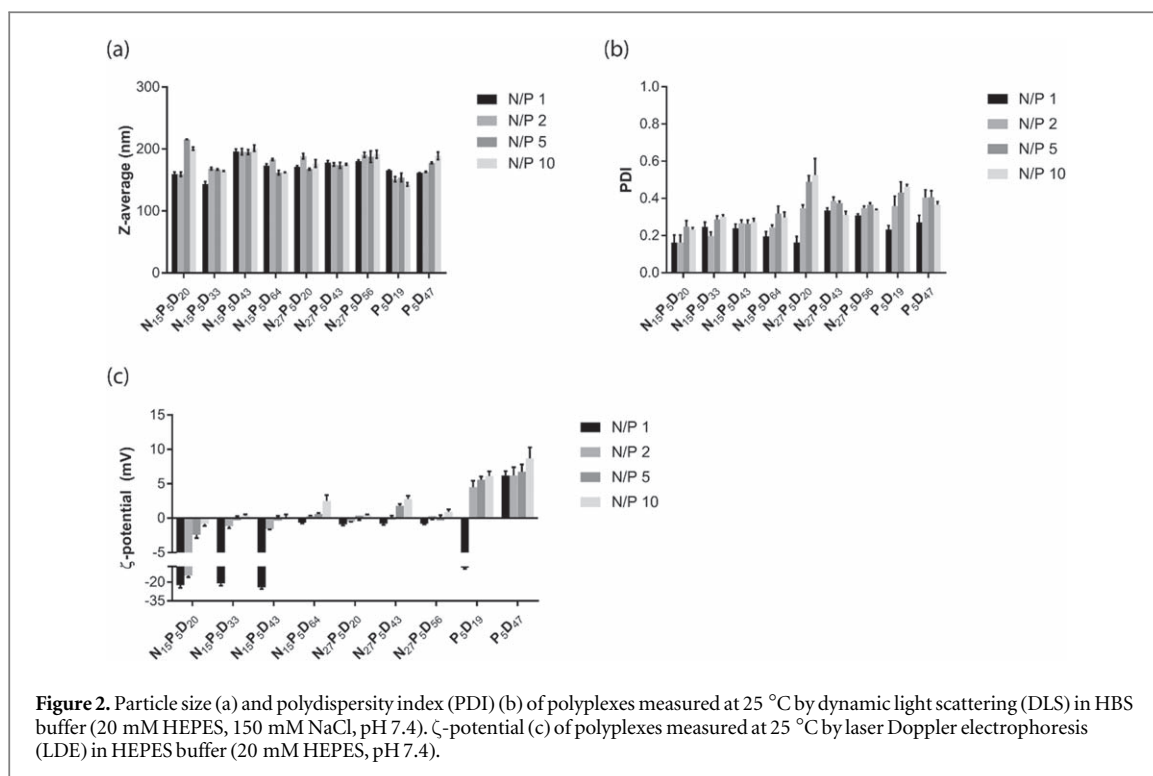
^b Determined by GPC.

^c Determined by light scattering at 550 nm. n.a. = not applicable.

PNIPAM has, almost independent of molecular weight and concentration, a CP of 32 °C in aqueous solutions, which makes it an attractive building block for biomedical and pharmaceutical materials [12, 13]. The CPs of the studied NPD polymers are 33 °C–34 °C (table 1 and figure S3), independent of cationic block lengths. Additionally, PD diblock copolymers lacking the thermosensitive PNIPAM block were synthesized, which served as control polymers in further experiments (figure 1(b)). Similar monomer conversion of DMAEMA and polymer yields were obtained, as for the NPD polymers (table 1, figure S2).

3.2. Polyplex formation and characterization at 25 °C

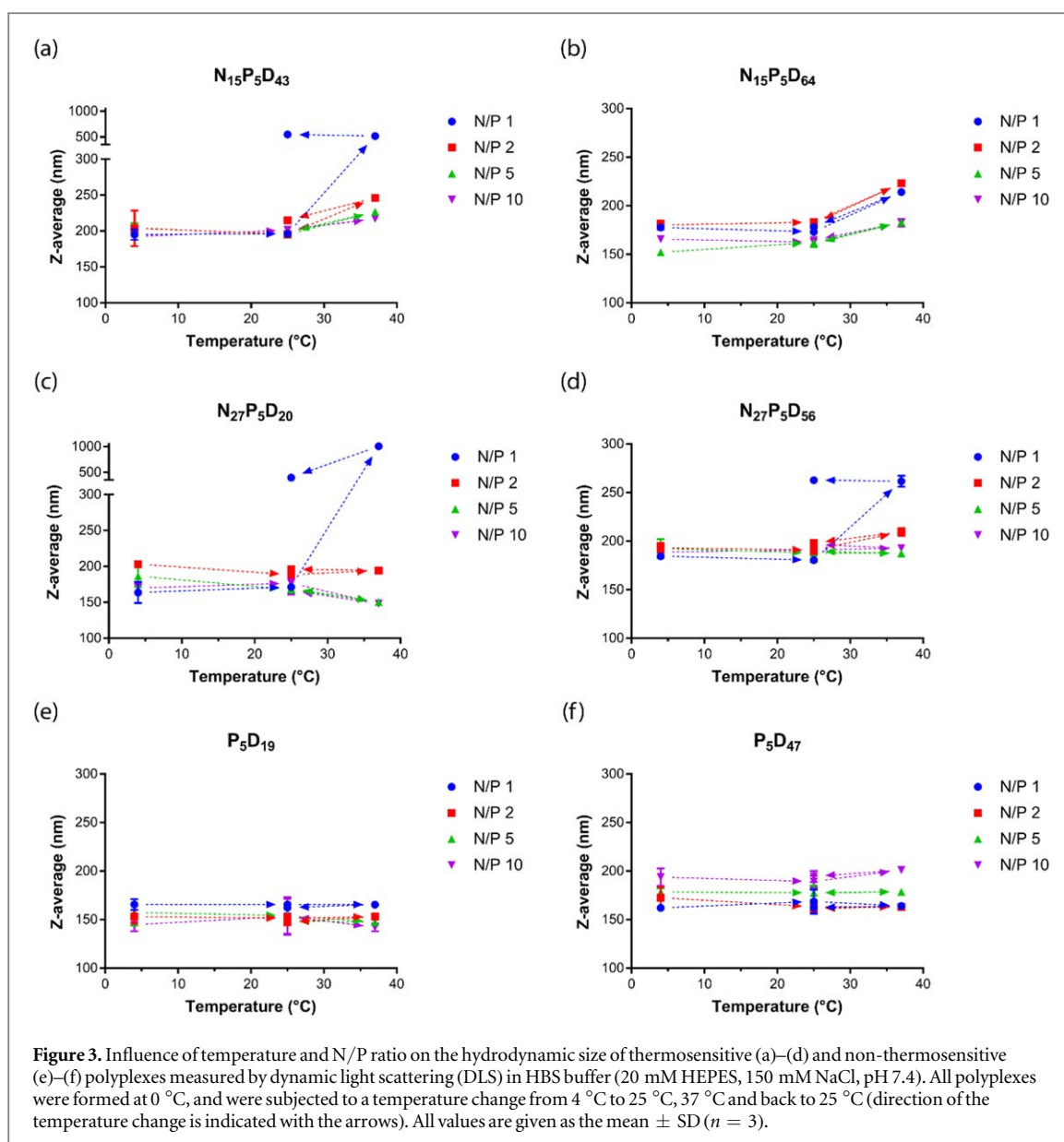
The effect of the NPD and ND composition on the formation of pDNA-based polyplexes (prepared at N/P ratios ranging from 1 to 10) was studied. The N/P ratio is defined as the molar ratio between the amine groups (N) on the cationic polymers and the phosphate groups (P) on the pDNA. The pDNA-loaded polyplexes were prepared at 0 °C, to allow the PNIPAM block to be fully hydrated, and afterwards the particles were characterized in terms of size and ζ -potential at 25 °C (figure 2). The hydrodynamic size of all polyplexes varied between 150 and 205 nm, and no clear trend between polymer composition and size of the polyplex was found. In addition, most polyplexes had acceptable PDIs ranging between 0.19 and 0.35 pointing to a narrow size distributions. In contrast, for N₂₇P₅D₂₀ and P₅D₁₉-based polyplexes high PDIs (>0.4) were observed with increasing N/P ratios. This is likely due to the short cationic block of the polymer, hampering effective condensation of the pDNA [32]. Furthermore, the ζ -potential of most NPD-polyplexes was neutral, indicating complete shielding of the surface charge. A previous study using random copolymers consisting of NIPAM and DMAEMA, showed that the ζ -potentials even at the maximum content of NIPAM (85 mol%) were all higher than 10 mV [16]. By separating the cationic block from the thermosensitive block in the NPD polymers, the charge of the polyplex was completely shielded by the PNIPAM-PEG blocks (both hydrophilic at 25 °C) even at high DMAEMA contents. Negative ζ -potentials were observed for a few polyplex dispersions prepared at a N/P < 2, suggesting incomplete complexation and condensation of the negatively charged pDNA. Indeed, these formulations also showed the presence of free pDNA bands in the agarose gel (figure S4). The absence of free pDNA bands in the agarose gel for all the other samples confirmed that all pDNA was complexed the polymer. Furthermore, upon



addition of the strongly negatively charged heparin, pDNA was released from the polyplexes showing that the complexation is reversible. PD-polyplexes had slightly positive ζ-potentials (ranging from 4.5–8.7 mV), which is in line with previous reported values for such polyplexes and significantly lower than non-PEGylated polyplexes [27, 32]. Further, the NPD polyplexes show a lower ζ-potential than the PD-based polyplexes, which is likely due to the additional shielding of the PNIPAM blocks. Taken all together, these data indicate that the presence of thermosensitive PNIPAM blocks of NPD does not hinder the electrostatic interactions between the cationic part of the polymers and pDNA, and thus the formation of stable polyplexes at 25 °C. Furthermore, the size of the polyplexes was not dependent on the molecular weight of the PNIPAM block (15 or 27 kDa).

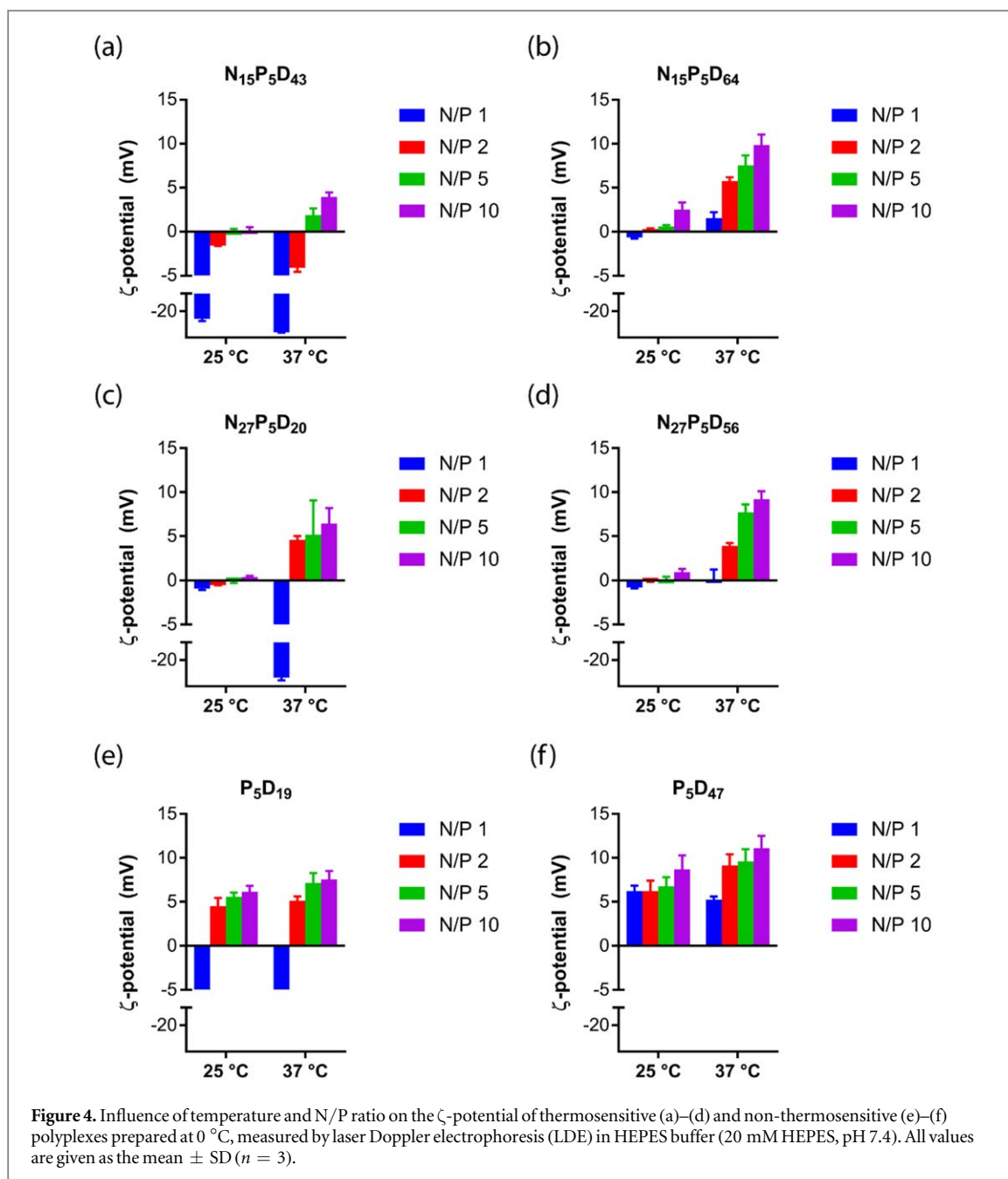
3.3. Polyplex stability at 37 °C

To investigate whether temperature-induced hydrophobic interactions changed the size and stability of the polyplexes, the polyplex dispersions were prepared at 0 °C (below the CP of NPD) followed by incubation at 37 °C (above the CP of NPD). First, the effect of temperature increase on the hydrodynamic size of polyplexes was studied. For this, polyplexes with various N/P ratios were formed at 0 °C, and subsequently heated from 4 °C to 25 °C and further to 37 °C. In addition, the polyplexes were cooled down again to 25 °C to assess the reversibility of temperature-induced change in hydrodynamic size. For all tested polyplex formulations, no significant changes in particle size were observed when the temperature was increased from 4 °C to 25 °C. This result is in line with expectations, as 25 °C is still below the CP of the thermosensitive polymers (33 °C–34 °C, table 1). When heated from 25 °C to 37 °C, polyplexes formed with the N₁₅P₅D₄₃ polymer at N/P 1 showed a significant increase in particle size from 195 to 516 nm which was non-reversible (figure 3(a)). Additionally, the ζ-potential of the polyplexes further decreased from –24.1 to –32.0 mV (figure 4(a)). The DLS results indicate that heating the sample above the CP of the polymer, results in irreversible aggregation of the polyplexes. However, this was not observed for polyplexes formed with the same polymer at higher N/P ratios (N/P of 2, 5 and 10). In addition, heating to 37 °C of polyplexes formed with polymers having longer cationic blocks from 43 to 64 kDa, did also not lead to irreversible aggregation at all tested N/P ratios (figure 3(B)). Polyplexes formed with polymers having a longer thermosensitive block (27 kDa) showed similar temperature-dependent behavior regarding particle size (figures 3(c)–(d)). The size of N₂₇P₅D₂₀-polyplexes only at N/P 1 was dramatically increased from 171 to above 1000 nm, when the temperature of the polyplex dispersion increased from RT to above the CP of the polymer. In addition, ζ-potential measurements showed a significant decrease in surface charge of N₂₇P₅D₂₀-polyplexes at this low N/P from neutral to –29.9 mV (figure 4(c)), clearly indicating exposure of pDNA. Increasing the cationic block length of the polymer from 20 to 56 kDa, still resulted in a significant increase in particle size after incubation at 37 °C (from 180 to 262 nm), whereas this was not the case for N₂₇P₅D₅₆-polyplexes at N/P ratios higher than 1. Interestingly, the ζ-potential of NPD-polyplexes, except for those formulations showing irreversible aggregation, increased when the temperature was changed from



25 °C to 37 °C. This might be explained by temperature-induced hydrophobic interactions between PNIPAM blocks present on the polyplex shell and free polymer chains. Subsequently, this can result in coating of the polyplex particle with free polymer chains having cationic PDMAEMA blocks on the outer shell. Especially at high N/P ratios, where not all polymer chains are expected to participate in the polyplex formation, this increase in ζ -potential is most evident. For example for $N_{15}P_5D_{64}$ -polyplexes, at N/P 1 the ζ -potential increases from -0.6 to 1.5 mV, whereas at N/P 10 the increase was from 2.5 to 9.9 mV (figure 4(b)). Moreover, interaction between free polymer chains and the polyplexes can also explain the slight temperature-dependent increase in hydrodynamic size observed for these polyplexes samples (from 162 to 183 nm), which was completely reversible (figure 3(b)). Interestingly, no effect of temperature-induced shrinking of PNIPAM on the polyplex size was observed. In order to attribute the observed changes in particle size during the temperature cycle to the presence of the thermosensitive block in the NPD polymers, non-thermosensitive PD polymers were included in this study as control. Only negligible temperature-induced changes in hydrodynamic size and ζ -potential were observed for PD-based polyplexes at all N/P ratios tested when exposed to the same changes in temperature (figures 3(e)–(f) and figures 4(e)–(f)). Overall, these results indicate that there is a critical balance between the electrostatic and hydrophobic interactions between the multifunctional polymer and pDNA at temperatures above the CP. To explain, when the length of the cationic block and the N/P ratio are high enough, the electrostatic interactions between the pDNA and the cationic block of the polymer are dominant over the hydrophobic thermosensitive interactions, resulting in sustaining the polyplex core structure (scheme 2).

To further investigate the balance between electrostatic and hydrophobic interactions, the preparation method of the polyplexes was changed from formation of the particles at 0 °C to formation at 37 °C. It is known



that NIPAM-based block copolymers with a permanent hydrophilic block, such as PEG, can self-assemble into micelles above their CP and their critical micelle concentration [33, 34]. Indeed, also the NPD polymers showed this self-assembly behavior into micellar structures at 37 °C, without the addition of pDNA (figure 5(a)). Sizes of the self-assembled micellar aggregates varied between 111–129 or 140–156 nm, when formed with polymers having a thermosensitive block length of 15 or 27 kDa, respectively. The relatively big size deviates from conventional core–shell micellar structures. However, the ζ -potentials of the micelles at pH 7.4 were all positive, ranging from 17.2 to 25.6 mV, indicating the formation of structures with a PNIPAM core and cationic PDMAEMA shell (figure 5(b)). To evaluate whether the formation of micelles influences the complexation between pDNA and the polymer, polyplexes were allowed to form upon addition of pDNA at 37 °C. Noteworthy, the polyplexes prepared at 37 °C displayed a slightly lower PDI value compared to polyplexes prepared at 4 °C suggesting that more uniform particles were formed in this preparation method. However, the same was observed for the PD diblock polymers, lacking the thermosensitive PNIPAM block, making this unlikely to be an effect of PNIPAM. No differences in hydrodynamic size at 25 °C were observed when the polyplexes were either formed at 0 °C or at a temperature above the polymer's CP (37 °C, figure 5(c)). These data suggest that thermosensitive hydrophobic interactions are dynamic enough to allow rearrangement of the structure to polyplexes upon addition of pDNA.

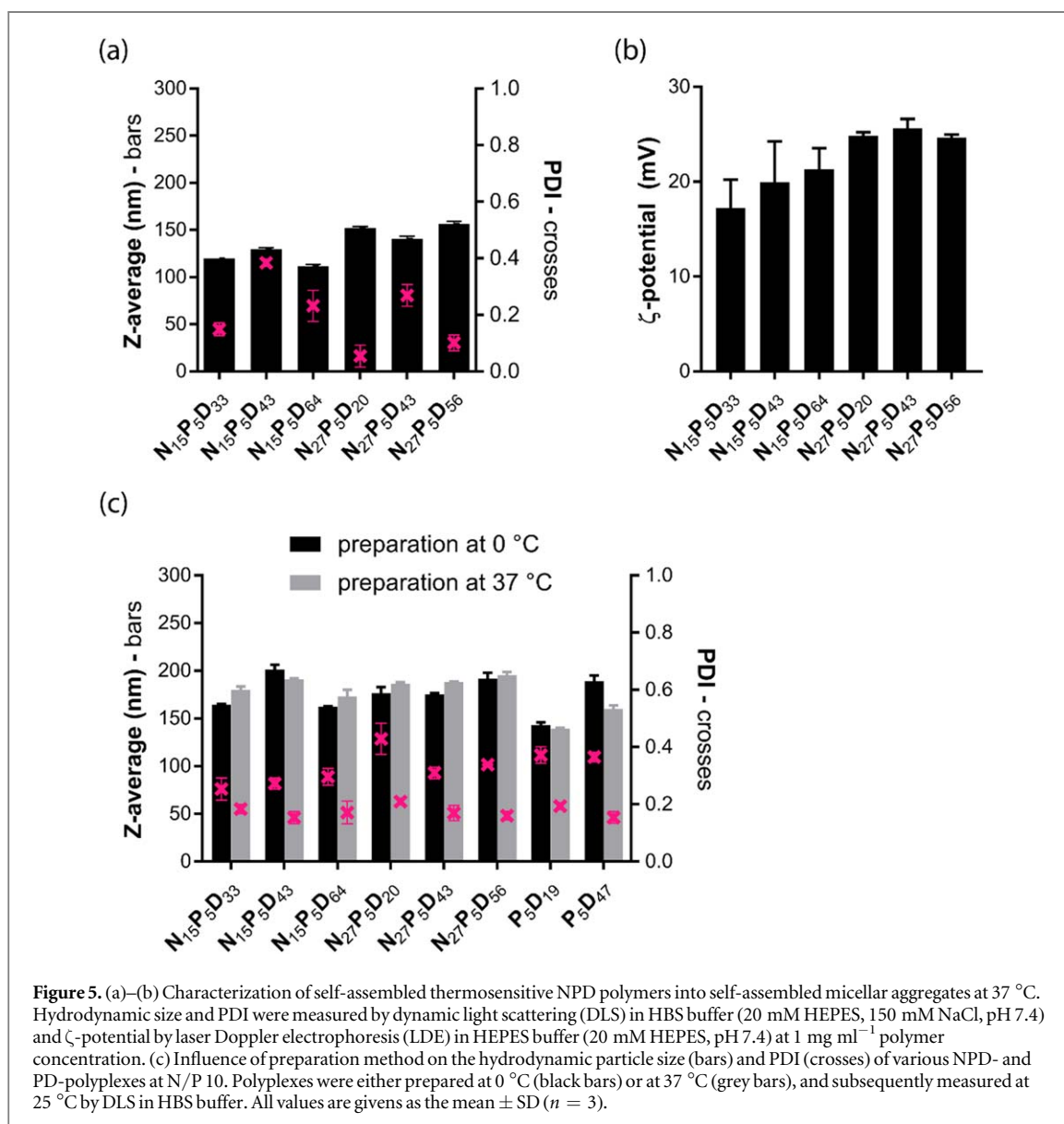
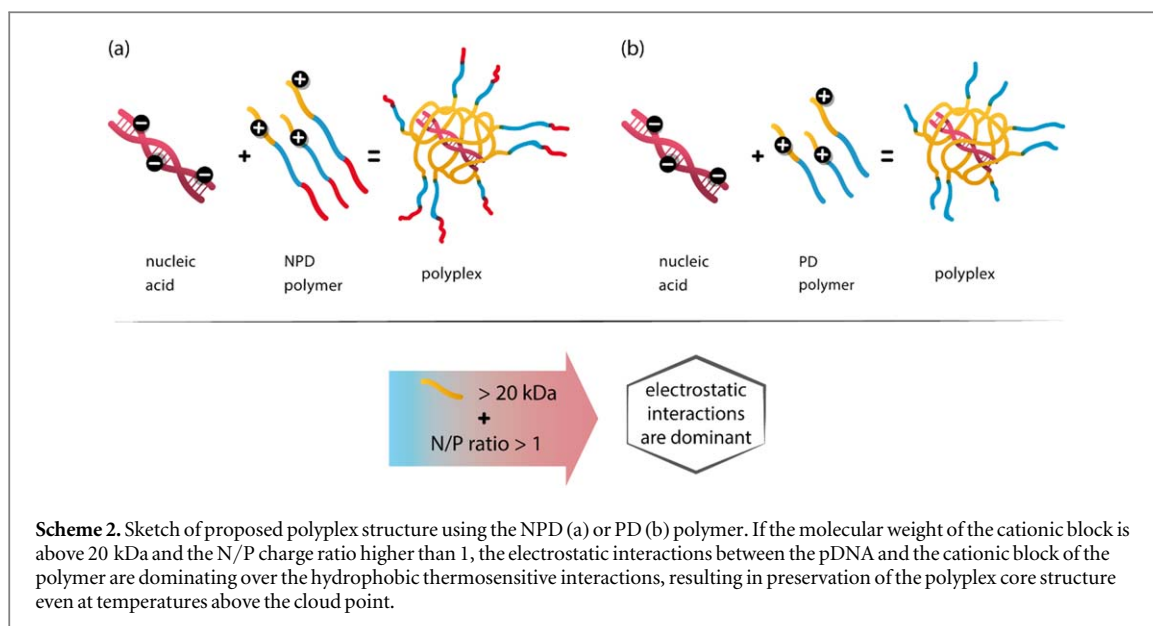


Table 2. Characteristics of $N_{15}P_5D_{43}$ - and P_5D_{47} -based polyplexes (N/P 5), and $N_{15}P_5D_{43}$ -based micelles measured at 10 °C and 37 °C by static light scattering (SLS) in HBS buffer (20 mM HEPES, 150 mM NaCl, pH 7.4).

Sample	Temperature (°C)	R_g (nm) ^a	R_h (nm) ^b	R_g/R_h
$N_{15}P_5D_{43}$ polyplex	10	125	87	1.4
	37	109	84	1.3
P_5D_{47} polyplex	10	135	85	1.6
	37	130	80	1.6
$N_{15}P_5D_{43}$ polymer	37	54	60	0.9

^a Radius of gyration extrapolated to zero concentration.

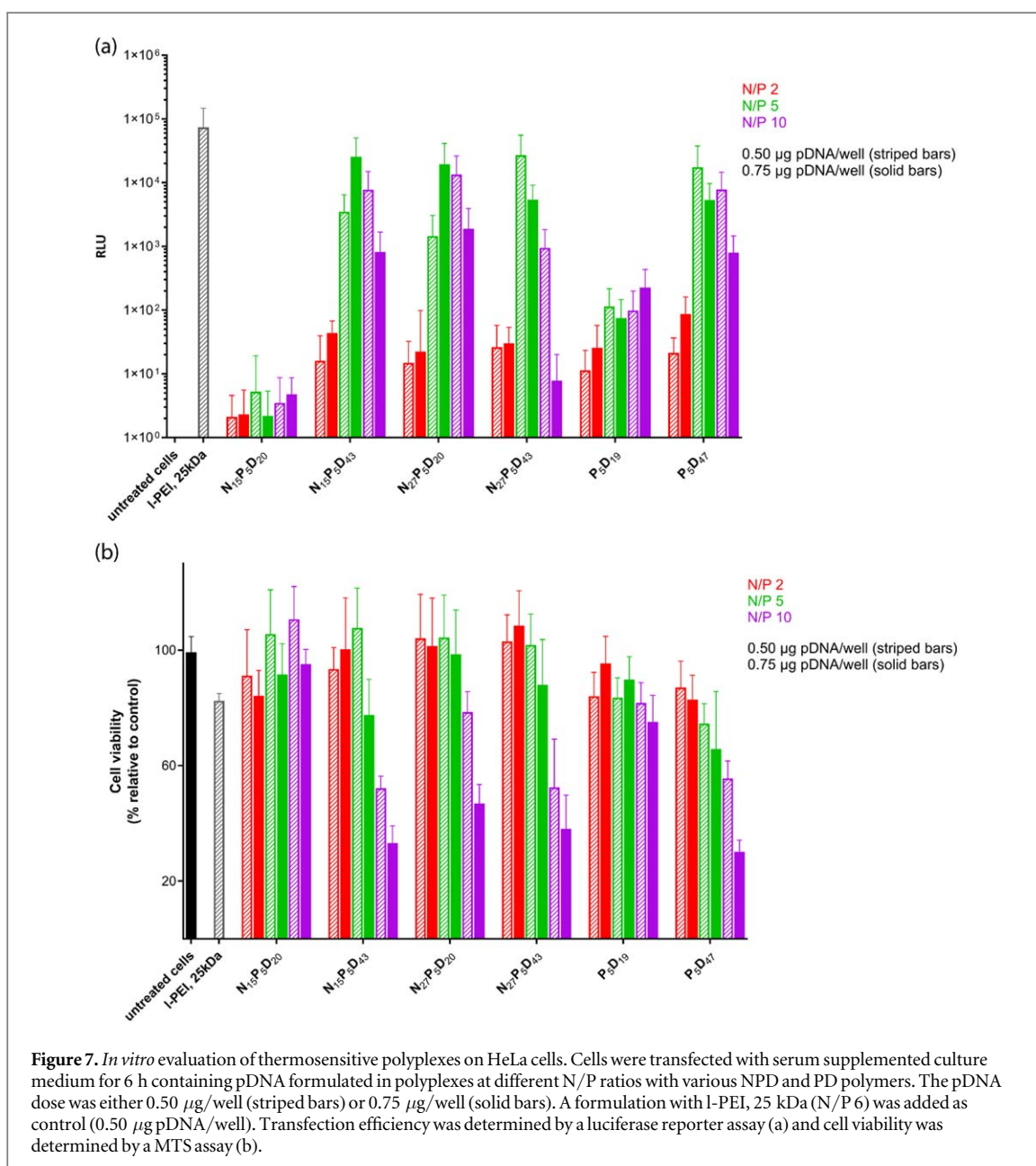
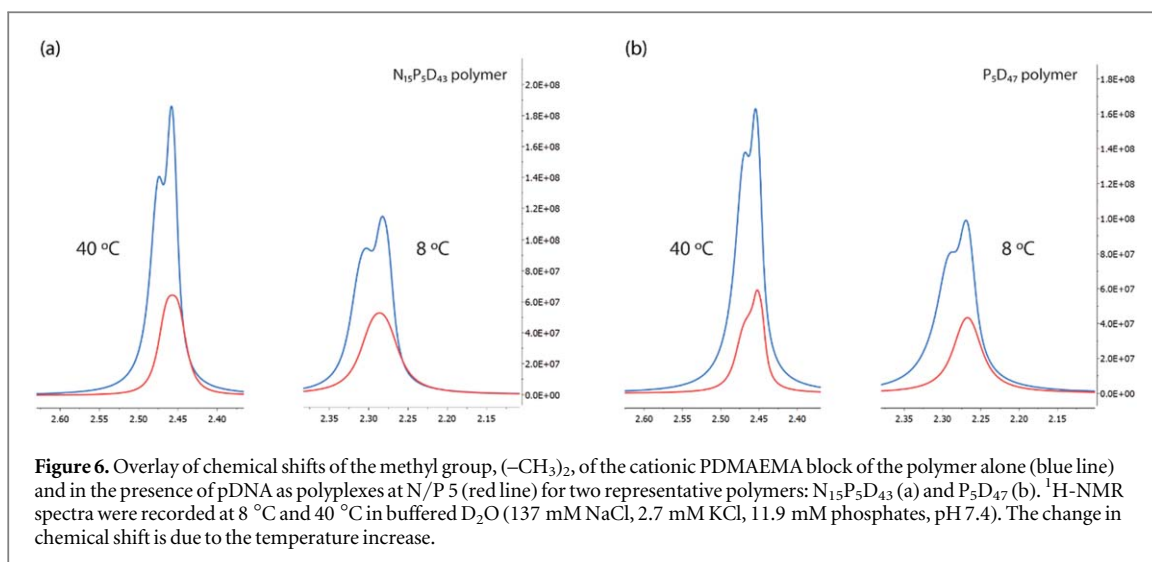
^b Hydrodynamic radius extrapolated to zero concentration and zero scattering angle.

Static light scattering measurements were performed to study the influence of temperature on the radius of gyration (R_g) and the hydrodynamic radius (R_h) of polyplexes. Polyplexes were prepared at N/P 5 with two representative polymers ($N_{15}P_5D_{43}$ and P_5D_{47}) having similar cationic block lengths. No substantial differences in R_g and R_h were observed for $N_{15}P_5D_{43}$ -polyplexes, when the temperature was increased from 10 to 37 °C (table 2). This is in agreement with the data obtained with DLS, as there were no significant changes in hydrodynamic size observed for the same polyplexes at this N/P ratio. In addition, the R_h values of the polyplexes found by SLS (80–87 nm) are in accordance with the hydrodynamic diameters measured by DLS (178–195 nm, figure 3). As expected, R_g and R_h values of polyplexes prepared with the control P_5D_{47} polymer did also not change in response to the temperature increase, which is in line with previous results (figures 3(e)-(f)). No significant differences in R_g/R_h ratio measured at 10 °C and 37 °C were observed for both polyplex samples (table 2). The ratio between R_g and R_h provides information about the shape and compactness of the particles. Changes in this ratio upon increasing the temperature above the polymer's CP can imply the possibility of morphological transformations of the polyplexes. These SLS data further support the finding that for polyplexes prepared at high N/P ratio for the $N_{15}P_5D_{43}$ triblock copolymer, the complex was stable upon the temperature change (figure 3). It is reported that for naked plasmid DNA having 5400 base pairs the R_g is ~210 nm and the R_g/R_h ratio ~1.8, in aqueous buffer solution with 150 mM NaCl [35, 36]. The lower values of both R_g and R_g/R_h ratio for the polyplexes samples, confirm the condensation of the DNA chains and the formation of particles, as reported before [36–38]. Furthermore, the R_g/R_h ratio found for the $N_{15}P_5D_{43}$ -polyplexes is very close to earlier reported values for PDMAEMA-based polyplexes [39]. Interestingly, a higher R_g/R_h ratio was found for P_5D_{47} -polyplexes, which could suggest a slightly different polyplex morphology. To explain, it has been shown in literature for example that PEGylated polyplexes can form rod like structures, which may explain the R_g/R_h ratio above 1 indicating non-spherical particles [40, 41]. In addition to the polyplexes, also the formation of $N_{15}P_5D_{43}$ -micelles (no addition of pDNA) at 37 °C was studied with SLS. Both R_g and R_h values were smaller than compared to those for the polyplex samples, as also shown by DLS. Moreover, the R_g/R_h ratio of 0.9 clearly indicates a more spherical-like structure of the micelles, which is in agreement with literature [33].

The polyplexes were studied by ¹H-NMR in D₂O below and above the CP of the thermosensitive polymer to investigate the electrostatic interactions between PDMAEMA and pDNA at different temperatures. At 8 °C, the signal corresponding to PDMAEMA at 2.3 ppm (methyl group, (–CH₃)₂) was suppressed upon the addition of pDNA compared to the signal of the polymer alone (figure 6). The decrease in intensity of this characteristic PDMAEMA signal confirmed the interaction with pDNA and the formation of polyplexes with decreased mobility of the PDMAEMA blocks. More importantly, suppression of the PDMAEMA signal was still observed when increasing the temperature above the polymer's CP, suggesting no change in the interaction of the PDMAEMA block and pDNA. The change in chemical shift at 40 °C as well as the more sharpened peaks are due to the temperature increase, which is most evident for the PDMAEMA signal without the presence of pDNA. Additionally, similar behavior was observed for the non-thermosensitive PD-polyplexes. The comparison here indicates that the presence of the PNIPAM blocks even at elevated temperatures does not change the local environment of protons of PDMAEMA. Furthermore, the signals corresponding to PNIPAM at 1.1 and 3.8 ppm were suppressed by increasing the temperature above the CP (figure S5–8). The disappearance of these characteristic signals confirmed that PNIPAM becomes dehydrated when heated above the CP [42].

3.4. *In vitro* transfection and cytotoxicity of thermosensitive polyplexes

The transfection efficiency and cytotoxicity of polyplexes based on NPD and PD polymers (table 1) were evaluated in the presence of serum using HeLa cells (figure 7). Increasing the N/P ratio for all type of polyplexes from 2 to 5 resulted in a higher transfection efficiency. However, a further increase of the N/P ratio to 10 did not lead to better transfection, which can be explained by the significant cytotoxicity observed for these polyplexes.



For the non-thermosensitive PD-based polyplexes, a higher transfection efficiency was observed with an increase in molecular weight of the cationic block from 20 to 47 kDa. However, this increased cationic block length of the polymer was also associated with a decrease in cell viability, which is in line with previous observations [32]. The same trend was observed for the thermosensitive NPD-based polyplexes, except for $N_{15}P_5D_{43}$ -based formulations prepared at N/P 10 which showed substantial cytotoxicity. Besides a transfection efficiency-dependence of the N/P ratio and cationic block length, a dose-dependent effect was observed as well. Increasing the pDNA dose from 0.50 to 0.75 $\mu\text{g}/\text{well}$ resulted in higher transfection efficiencies, however, it was also associated with more cytotoxicity. These findings are not surprising, since it has been reported for cationic polymers that transfection efficiency and cytotoxicity depend on molecular weight of the polymer, surface charge of the polyplex and dose [43, 44]. Interestingly, NPD-based polyplexes show better cytocompatibility than PD-based ones with similar cationic block lengths, even at the lower N/P ratios of 2 and 5. This can be explained by a difference in surface charge of the polyplexes at 37 °C. As shown in figure 4, the NPD polyplexes had a lower ζ -potential than the PD-based polyplexes, which is likely due to the additional shielding of the PNIPAM blocks. For example, at 37 °C $N_{15}P_5D_{43}$ -polyplexes with N/P 5 had a ζ -potential of 1.9 ± 0.7 mV, while the P_5D_{47} -polyplexes showed a ζ -potential of 9.6 ± 1.4 mV. When comparing $N_{15}P_5D_{20}$ -based polyplexes with $N_{27}P_5D_{20}$ -based ones, it can be seen that an increase of the PNIPAM molecular weight from 15 to 27 kDa resulted in significantly higher transfection efficiencies. However, such a trend was not seen between $N_{15}P_5D_{43}$ - and $N_{27}P_5D_{43}$ -based polyplexes. It might be that this effect of PNIPAM is diminished by the increased cytotoxicity observed for higher cationic block lengths.

As a control, a PEI formulation was included which showed about 3–10 times higher transfection compared to NPD or PD formulations. However, a decrease in cell viability was observed for this formulation as well. The increased transfection efficiency is not uncommon when PEI is compared with PEGylated polyplexes, which are normally taken up to a lower extent than polyplexes based on unmodified cationic polymers (such as PEI) [26, 45, 46]. Such formulations are however not suitable for *in vivo* applications and local administration of non-PEGylated polyplexes is known to result in low transfection because of their restricted mobility [27, 47].

In conclusion, these results suggest that the presence of thermosensitive blocks in NPD-based polyplexes resulted in better cytocompatibility compared to PD-based polyplexes with similar efficiencies of delivering its cargo into HeLa cells. and The cytotoxicity-transfection efficiency balance is not only determined by the cationic block, but also the effect of PNIPAM should be considered in designing thermosensitive polyplexes.

4. Conclusion

Cationic block copolymers based on PDMAEMA, PEG and PNIPAM formed complexes with plasmid DNA under physiologically relevant conditions. The results show that there is a critical balance between the electrostatic and hydrophobic interactions between the multifunctional polymer and pDNA at temperatures above the CP. If the length of the cationic block is higher than 20 kDa and the N/P charge ratio higher than 1, the electrostatic interactions between the pDNA and the cationic block of the polymer are dominating over the hydrophobic thermosensitive interactions, resulting in preservation of the polyplex core structure. Moreover, the introduction of PNIPAM in a block-like structure to cationic polymers enables formation of polyplexes with pDNA that shield the charge of the polyplexes to a much larger extent than PEG diblock copolymers at physiological temperature. The thermosensitive polyplexes showed improved cytocompatibility compared to the non-thermosensitive polyplexes at all tested N/P ratios, which might be a result of the enhanced surface-charge shielding. Furthermore, transfection experiments indicated that all polymers used in this study were able to deliver their cargo in HeLa cancer cells even in the presence of serum proteins. Overall, we showed that by careful tuning lengths of polymer blocks different properties can be introduced without compromising the polyplex structure with pDNA. This strategy has potential for different applications, of which an example could be the use of the thermosensitive blocks to anchor polyplexes in a thermosensitive hydrogel for the controlled and local delivery of nucleic acids.

Acknowledgments

We gratefully acknowledge K Houben (Utrecht University) for the assistance with the experiments on the Bruker 500 MHz NMR spectrometer and R G Fokkink (Wageningen University and Research) for the help with the static light scattering experiments. The Netherlands Organization for Scientific Research (NWO/VIDI 13457 and NWO/Aspasia 015.009.038) is acknowledged for funding.

ORCID iDs

Tina Vermonden  <https://orcid.org/0000-0002-6047-5900>

References

- [1] Chakraborty C, Sharma A R, Sharma G, Doss C G P and Lee S-S 2017 *Mol. Ther. - Nucl. Acids* **8** 132–43
- [2] Merkel O M and Kissel T 2014 *J. Control. Release* **190** 415–23
- [3] Lachelt U and Wagner E 2015 *Chem. Rev.* **115** 11043–78
- [4] Agarwal S, Zhang Y, Maji S and Greiner A 2012 *Mater. Today* **15** 388–93
- [5] Wagner E 2014 *Adv. Genet.* **88** 231–61
- [6] Lazzari M and López-Quintela M A 2003 *Adv. Mater.* **15** 1583–94
- [7] Cohen Stuart M A et al 2010 *Nat. Mater.* **9** 101
- [8] Sun H, Kabb C P, Sims M B and Sumerlin B S 2019 *Prog. Polym. Sci.* **89** 61–75
- [9] Alarcon C D H, Pennadam S and Alexander C 2005 *Chem. Soc. Rev.* **34** 276–85
- [10] Bordat A, Boissenot T, Nicolas J and Tsapis N 2019 *Adv. Drug. Deliv. Rev.* **138** 167–92
- [11] Fu X, Hosta-Rigau L, Chandrawati R and Cui J 2018 *Chem* **4** 2084–107
- [12] Najafi M, Hebels E, Hennink W E and Vermonden T 2018 *Temperature-Responsive Polymers: Chemistry, Properties, and Applications* ed V V Khutoryanskiy and T K Georgiou (New York: Wiley) ch 1 pp 3–34
- [13] Schild H G 1992 *Prog. Polym. Sci.* **17** 163–249
- [14] Alexander C 2006 *Expert Opin. Drug Deliv.* **3** 573–81
- [15] Yokoyama M 2002 *Drug Discovery Today* **7** 426–32
- [16] Hinrichs W L J, Schuurmans-Nieuwenbroek N M E, van de Wetering P and Hennink W E 1999 *J. Control. Release* **60** 249–59
- [17] Kurisawa M, Yokoyama M and Okano T 2000 *J. Control. Release* **69** 127–37
- [18] Kurisawa M, Yokoyama M and Okano T 2000 *J. Control. Release* **68** 1–8
- [19] Twaites B R, Alarcon C D, Cunliffe D, Lavigne M, Pennadam S, Smith J R, Gorecki D C and Alexander C 2004 *J. Control. Release* **97** 551–66
- [20] Twaites B R, Alarcon C D H, Lavigne M, Saulnier A, Pennadam S S, Cunliffe D, Gorecki D C and Alexander C 2005 *J. Control. Release* **108** 472–83
- [21] Wei M, Gao Y, Li X and Serpe M J 2017 *Polym. Chem.* **8** 127–43
- [22] Garbern J C, Hoffman A S and Stayton P S 2010 *Biomacromolecules* **11** 1833–9
- [23] de Graaf A J, Azevedo Prospero dos S I I, Pieters E H, Rijkers D T, van Nostrum C F, Vermonden T, Kok R J, Hennink W E and Mastrobattista E 2012 *J. Control. Release* **162** 582–90
- [24] Fliervoet L A L, Engbersen J F J, Schiffelers R M, Hennink W E and Vermonden T 2018 *J. Mater. Chem. B* **6** 5651–70
- [25] Wang L L and Burdick J A 2017 *Adv. Healthcare Mater.* **6** 1601041
- [26] Malek A, Czubayk F and Aigner A 2008 *J. Drug Targeting* **16** 124–39
- [27] Verbaan F J, Oussoren C, Snel C J, Crommelin D J A, Hennink W E and Storm G 2004 *J. Gene Med.* **6** 64–75
- [28] Lisitsyna E S, Ketola T M, Morin-Picardat E, Liang H M, Hanzlikova M, Urtti A, Yliperttula M and Vuorimaa-Laukkanen E 2017 *J. Phys. Chem.* **121** 10782–92
- [29] Fliervoet L A L, Najafi M, Hembury M and Vermonden T 2017 *Macromolecules* **50** 8390–7
- [30] Moore J S and Stupp S I 1990 *Macromolecules* **23** 65–70
- [31] van Gaal E V, van Eijk R, Oosting R S, Kok R J, Hennink W E, Crommelin D J and Mastrobattista E 2011 *J. Control. Release* **154** 218–32
- [32] van de Wetering P, Cherng J Y, Talsma H and Hennink W E 1997 *J. Control. Release* **49** 59–69
- [33] de Graaf A J et al 2011 *Langmuir* **27** 9843–8
- [34] Topp M D C, Dijkstra P J, Talsma H and Feijen J 1997 *Macromolecules* **30** 8518–20
- [35] Araki S, Nakai T, Hizume K, Takeyasu K and Yoshikawa K 2006 *Chem. Phys. Lett.* **418** 255–9
- [36] Dai Z J and Wu C 2012 *Macromolecules* **45** 4346–53
- [37] He E, Yue C Y, Simeon F, Zhou L H, Too H P and Tam K C 2009 *J. Biomed. Mater. Res. A* **91A** 708–18
- [38] Tan J F, Too H P, Hatton T A and Tam K C 2006 *Langmuir* **22** 3744–50
- [39] You Y Z, Manickam D S, Zhou Q H and Oupicky D 2007 *J. Control. Release* **122** 217–25
- [40] Takeda K M, Osada K, Tockary T A, Dirisala A, Chen Q and Kataoka K 2017 *Biomacromolecules* **18** 36–43
- [41] Tockary T A, Osada K, Motoda Y, Hiki S, Chen Q X, Takeda K M, Dirisala A, Osawa S and Kataoka K 2016 *Small* **12** 1193–200
- [42] Najafi M, Kordalivand N, Moradi M A, van den Dikkenberg J, Fokkink R, Friedrich H, Sommerdijk N, Hembury M and Vermonden T 2018 *Biomacromolecules* **19** 3766–75
- [43] Samsonova O, Pfeiffer C, Hellmund M, Merkel O M and Kissel T 2011 *Polymers* **3** 693–718
- [44] Yue Y A, Jin F, Deng R, Cai J G, Dai Z J, Lin M C M, Kung H F, Matthebjerg M A, Andresen T L and Wu C 2011 *J. Control. Release* **152** 143–51
- [45] Fella C, Walker G F, Ogris M and Wagner E 2008 *Eur. J. Pharm. Sci.* **34** 309–20
- [46] Raup A, Wang H, Synatschke C V, Jerome V, Agarwal S, Pergushov D V, Muller A H and Freitag R 2017 *Biomacromolecules* **18** 808–18
- [47] van den Berg J H, Oosterhuis K, Hennink W E, Storm G, van der Aa L J, Engbersen J F J, Haanen J B A G, Beijnen J H, Schumacher T N and Nuijen B 2010 *J. Control. Release* **141** 234–40